Topography, SST anomalies, and precipitation: Unveiling Cyclogenesis in South America

UtahState University
PLANTS, SOILS & CLIMATE

Dr. Luthiene Dalanhese

Introduction

Chang (2017) highlights that climate change may bolster the potential for extreme extratropical cyclones adjacent to South America, and more knowledge about the observed characteristics of ECs is needed. The South America climatology and characteristics of cyclogenesis have been explored in the past few years by Gramcianinov et al. (2020), Hoskins and Hodges (2005), Murray and Simmonds (1991), Sinclair (1994), and others used automatic schemes to understand cyclonic behavior over Southern Hemisphere. With South America in the spotlight, Crespo et al. (2021), (Gozzo et al. (2017, 2014), Reboita et al. (2018, 2010), Rocha et al. (2016) use regional models to understand the cyclogenetic characteristics of regions close to the coast. Both Crespo et al. (2021) and Gramcianinov et al. (2019) point in their results lee of the Andes as a cyclogenetic region, confirming the findings of (Gan and Rao, 1994).

Conclusion

A seesaw pattern in South American cyclogenesis Lee and coastal cases exhibit opposite behaviors possibly triggered by SST variances. Lee cyclogenesis correlates with negative Pacific SST anomalies, while coastal cyclogenesis intensifies with warmer Pacific anomalies. Coastal cyclones increase under positive SST conditions in the South Atlantic due to enhanced atmospheric instability near the coast. Vortex stretching and vorticity advection contribute to coastal cyclogenesis, indicating potential forecasting benefits by considering ENSO, cross-basin SST differences, and upper tropospheric features.

Results

Fig. 01

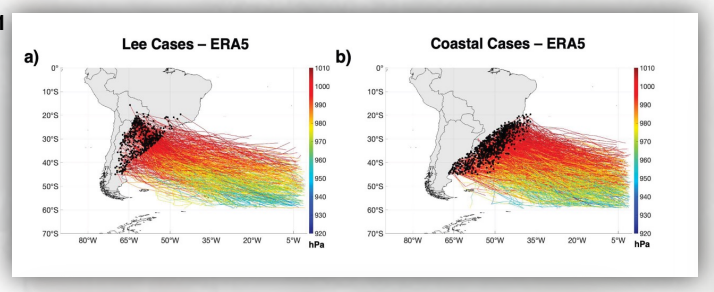

Fig. 01 - Genesis locations (shown in black dots) of lee (a and c) and coastal (b and d) extratropical cyclones along with storm tracks for ERA5 reanalysis (a,b). The pressure is given in hectopascal (hPa).

Fig. 02 - Time series of the frequency of ERA5 ECs for lee (red line) and coastal (blue line) cyclogenesis in a calendar year (July-June). On the left-hand side are the genesis values for coastal cases, and on the right-hand side is the number of geneses for lee cases. Blue (red) shaded colors indicate selected years for a high number of coastal (lee) area cases.

Fig. 03 - Composite stream function anomalies (contours) and SST anomalies (shading) for years with high and low frequencies of lee cyclogenesis (a, b, respectively) and high and low frequencies of coastal cyclogenesis (c, d respectively). Positive (negative) stream function values in the Southern Hemisphere indicate a cyclonic (anticyclonic) anomaly or a low (high) pressure area. Blue (purple) dots represent cyclogeneses in the coastal (lee) area during the selected years, where each dot represents a cyclone during this period. Arrows were manually added to allow wind direction reference.

Fig. 04 - Composite stream function anomalies - 850 hPa - (contours) and total precipitation anomalies (shading) for years with high and low frequencies of lee cyclogenesis (a, b, respectively) and high and low frequencies of coastal cyclogenesis (c, d respectively). Positive (negative) stream function values in the Southern Hemisphere indicate a cyclonic (anticyclonic) anomaly or a low (high) pressure area. Blue (purple) dots represent cyclogeneses in the coastal (lee) area during the selected years, where each dot represents a cyclone during this period.

Fig. 05 - Composite stream function anomalies (contours) and specific humidity anomalies (shading) – both 850 hPa - for years with high and low frequencies of lee cyclogenesis (a, b, respectively) and high and low frequencies of coastal cyclogenesis (c, d respectively). Positive (negative) stream function values in the Southern Hemisphere indicate a cyclonic (anticyclonic) anomaly or a low (high) pressure area. Blue (purple) dots represent cyclogeneses in the coastal (lee) area during the selected years, where each dot represents a cyclone during this period. Arrows were manually added to allow wind direction reference.

Fig. 06 - *Sections of vorticity advection $[V, -V \cdot \nabla(f + \zeta)]$ and vortex stretching $[(f + \zeta)\nabla \cdot V]$ (shaded $[x10^{-11} m^2 s^{-1}]$) are presented. Vorticity advection analysis (figure 9a, c) averaged for the upper troposphere (500 hPa) across 38°S 24°S with 500 hPa wind vectors. Vortex stretching analysis (figure 9b, d) or the lower troposphere from 850–500 hPa across 38°S 24°S for lee cases (figure 9b) and from 1000–850 hPa for coastal cases (figure 9d) with 850 hPa wind vectors [m/s]. Blue (purple) dots represent cyclogeneses in the coastal (lee) area during the selected years. A map of South America evidencing the Andes Mountains is plotted to provide a geographical reference.*

Fig. 03

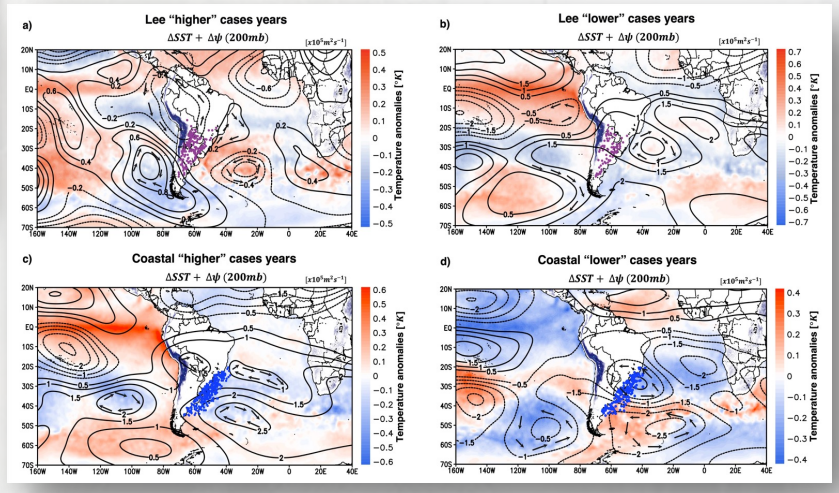

Fig. 02

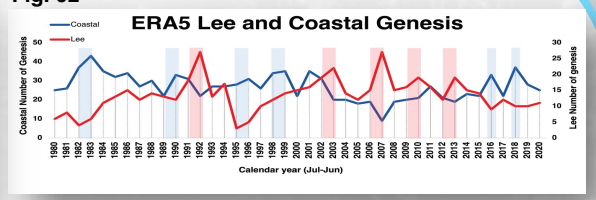

Fig. 04

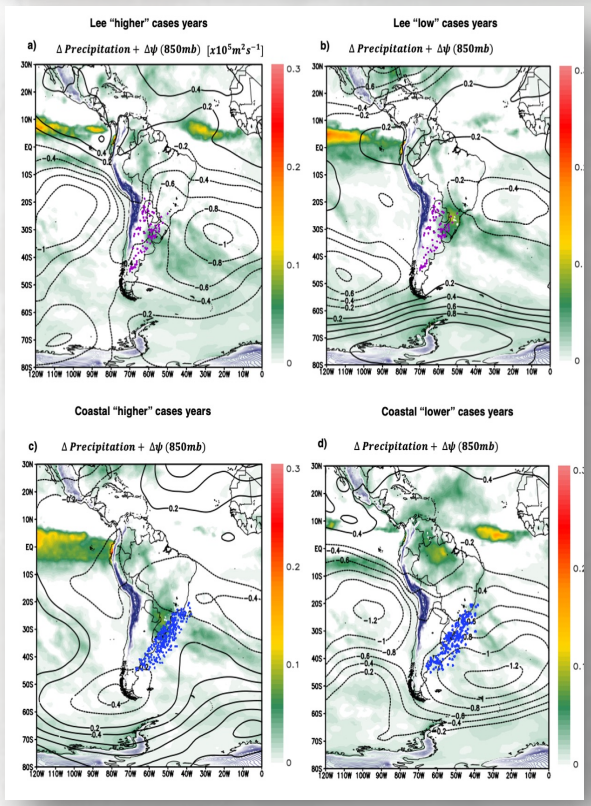

Fig. 05

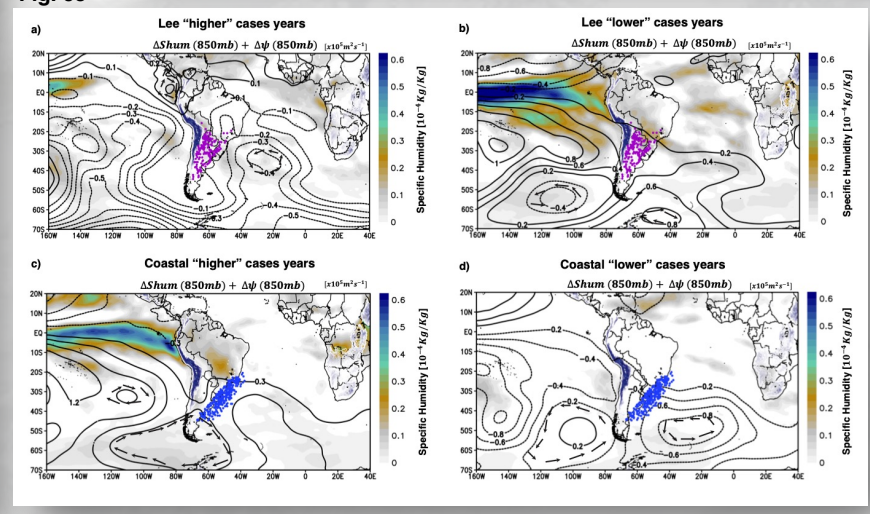

Fig. 06